

Effect of low initial pressures on ignition properties of methane/O₂/N₂ mixtures for laser induced breakdown

Bastien MOLIERE, Steve RUDZ, Jérémy DOUGAL,
Philippe GILLARD, Mame WILLIAM-LOUIS

Univ. Orléans, INSA-CVL, Laboratoire PRISME EA 4229 IUT de Bourges, 63 Avenue du
Maréchal de Lattre de Tassigny, 18020 BOURGES, FRANCE.

1 Introduction

Increasing engines performances, while cutting down manufacturing and maintenance costs, fuel consumption and exhaust emissions, are one of the main issues of the aerospace industry. Studied for the first time in the early sixties, aerospace propulsion is witnessing a renewed interest in laser-induced spark ignition, for the last twenty years, because of many potential benefits over conventional electrical ignition systems. Laser-induced breakdown allows an accurate control of the input energy, that is, the energy absorbed by the oxidizer/fuel mixture. Thanks to a more stable combustion than spark plug, laser ignition provides a lower fuel consumption and a decrease in polluting emissions in transportation systems [1]. Ignition is also made easier for lean fuel mixture and for high and low pressures mixtures [2,3]. Furthermore, laser ignition extends the lean flammability limit, compared with spark ignition [4]. In order to reduce NO_x emissions, the strategy using lean mixtures leads to a slow speed of flame front inside the cylinder, which causes a rise of the heat loss and the reduction of the thermal efficiency. Laser-induced multi-point ignition triggers the ignition of several sites inside the cylinder. As the total burning time throughout the mixture volume is smaller, the multiple flame fronts don't have the time to lose heat, the thermal efficiency is improved [3]. Similarly, multi-point ignition can act as a substitute for the turbulence rate established by the combustion chamber design, both factor of mixing and heat losses [3]. One other obvious asset of laser ignition is the non-intrusive aspect offered by this device. Except for a window allowing the laser beam to enter the combustion chamber, an electrode-less ignition does not disturb the cylinder geometry, and above all, gets rid of problems such as quenching effect on flame kernel (heat loss through the electrodes) [5]. The elimination of kernel cooling and the reduction of ignition delay time could also enhance the combustion stability at high Mach and facilitate the flight at lower dynamic pressures requested for hypersonic flight systems [5]. In the operational framework, its features could be a milestone to simplify the maintenance and improving performances of actual and future aviation engines [5]. This paper presents the ignition energy of methane and synthetic air, by laser-induced spark, at low initial pressures. This parametric study on equivalence ratio and pressure aims at finding a law for the absorbed energy. Often regarded as a "clean" fuel, methane emerges as a promising alternative to kerosene or hydrogen used as propellant in the space industry [6]. Such a study may also be useful for safety considerations [7] as flammability limits are explored.

2 Experimental apparatus

Figure 1 describes the apparatus used through a schematic view of the experimental set-up. The combustion chamber is a cylindrical vessel heated up to 303 K (30 °C) with a length of 200 mm and an internal diameter of 80 mm (1 Litre). The methane (>99,95% purity) and the synthetic air (20% O₂ and 80% N₂) are injected in the vessel by means of a manometer after establishment of primary vacuum. The Gaussian laser beam used is generated by a Quantel Brilliant Q-switched Nd:Yag ($\lambda = 1064$ nm, $D = 6$ mm, $M^2 = 1.75$, pulse duration -Full Width at Height Maximum- $\tau = 4.48$ ns) with a laser incident energy adjustable up to 300 mJ. Combined with an optical system of lenses, the laser beam is focalized into the vessel to achieve a breakdown. Firstly, the beam laser is expanded by a factor of 3 thanks to the plano-concave lens L1 and the plano-convex lens L2. Then, the pyroelectric energy meter J1 measures 5% of the input energy (incident beam) thanks to a beam splitter. Lastly, the remainder of the beam is focused in the center of the vessel with the plano-convex lens L3 ($f_3 = 150$ mm) and the output energy (transmitted beam) is determined by the energy meter J2.

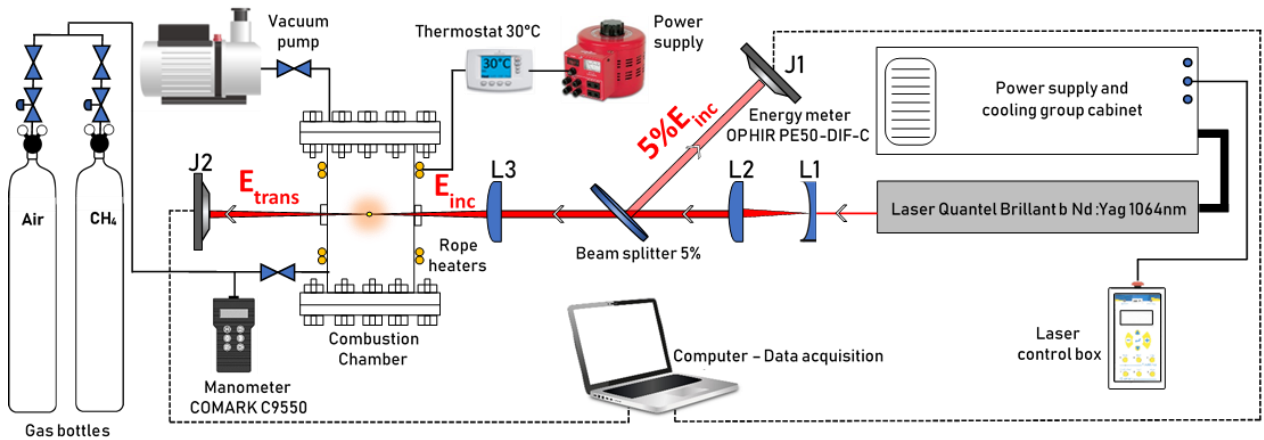


Figure 1. Schematic view of the experimental set-up: Laser Ignition QUIescent Mixtures (LIQUIM) test bench

3 Experimental protocol

In this work, ten equivalence ratios Φ from 0.20 to 1.40 at initial temperature and pressures of 303 K and from 200 mbar to 795 mbar respectively are investigated. To deal with each successful configurations, we use the Langlie method [8] with a log-normal law. This statistical approach generally needs only 20-25 shots to provide a valid empirical relation between incident energy and ignition probability [9]. Essentially, this method employs a dichotomy approach to spot the raw E_{50} , the incident energy needed to obtain an ignition probability of 50 %, and calculates the corresponding raw standard deviation σ_0 :

$$\text{raw } E_{50} = (X_m + X_M) / 2 \quad \text{and} \quad \sigma_0 = N(\ln(X_m) - \ln(X_M)) / 8(n + 2) \quad (1)$$

where X_m is the lowest energy leading to ignition, X_M the highest energy leading to no-ignition, N the total number of shots and n the number of shots occurred between $[X_m; X_M]$.

A fitting equation of experimental results to the cumulative distribution function of a log-normal law is:

$$F_{\log}(E) = \left(1 + \text{erf}\left(\frac{(\ln(E) - \mu)}{\sqrt{2}\sigma}\right)\right) / 2 \quad (2)$$

where μ and σ are respectively the mean and the standard deviation of the energy. Finally, we can calculate the corrected value of energy:

$$E_{50} = \exp(\mu) \quad (3)$$

4 Results and discussions

E₅₀ measurements

The estimated energy E_{50} for CH₄/Air (20% O₂, 80% N₂) mixtures are reported in Table 1, as a function of the total pressure P_{tot} initially in the chamber and the mixture equivalence ratio Φ . The blank fields have been tested but manifested no observable ignition, even with the maximum incident energy adjustable.

Table 1: E_{50} [mJ] referred to the different investigated conditions (P_{tot} [mbar]; Φ).

$P_{tot} \backslash \Phi$	0.2	0.3	0.4	0.5	0.6	0.75	0.9	1	1.07	1.15	1.24	1.40
200		89.1	58.7	54.6	48.1	70.6	142.4					
325		63.6	31.0	19.8	23.2	24.6	27.5	96.4	121.3			
452.7		43.6	23.6	13.9	15.9	16.0	16.0	28.2	30.1	47.0	104.3	
616.4			25.0	10.2	13.8	12.4	11.1	14.5	15.7	24.4	81.8	
795			24.7	10.3	10.3	8.9	9.4	9.0	9.5	19.0	38.1	

Figure 2 reveals the U-shaped trend of E_{50} with equivalence ratio, for different low pressures. The figure displays the error bars according to the equivalent ratio and the E_{50} . The E_{50} decreases, when the pressure increases. If the minimum E_{50} is focused at 0.6 for 200 mbar, for the other pressures, it appears to remain constant from the equivalent ratio 0.5 to a value increasing with the pressure (from 0.9 to 1.07). The E_{50} drastically decreases between 200 and 325 mbar and the E_{50} steeply increases between the equivalence ratios 1.15 and 1.24.

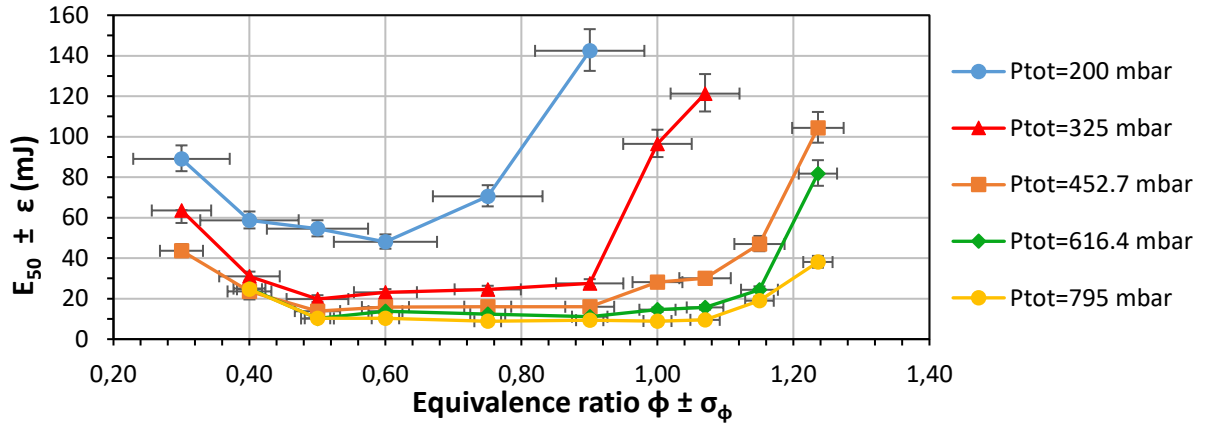


Figure 2. E_{50} [mJ] vs equivalence ratio Φ for different initial vessel pressures P_{tot} [mbar]

Empirical modeling of energy deposit

In a previous work [10] the energy deposit E_{abs} was satisfyingly modelled for laser-induced ignition of n-decane/air mixtures for initial pressures P_{tot} of the same range through the following power law:

$$E_{abs} = \alpha (E_{inc} - \beta)^\delta \quad (4)$$

where α and δ are dimensionless constants and β is a constant with the dimension of an energy.

Physically, β can be considered as a minimum threshold energy to achieve a breakdown and α can be considered as the maximum fraction of absorbed energy. A noticeable result in [10] is that E_{abs} was not correlated to Φ and the energy deposit was linear (*i.e.* $\delta = 1$).

Figure 3 points out the low-dependence of energy absorption on equivalence ratio. At a given pressure and for all reviewed equivalence ratio (3.a), the fitting curves are significantly close: the amount of absorbed energy is comparable. In contrast, at a given equivalence ratio and for all considered pressures (3.b), the amount of absorbed energy is dissimilar. As a result, only P_{tot} is taken into consideration to describe the fluctuations of absorbed energy, and no more Φ : the constants (α , β , δ) are supposed as function of the pressure. At a given P_{tot} (3.a), we can consider the average of the fitting curves regardless of Φ (4.a).

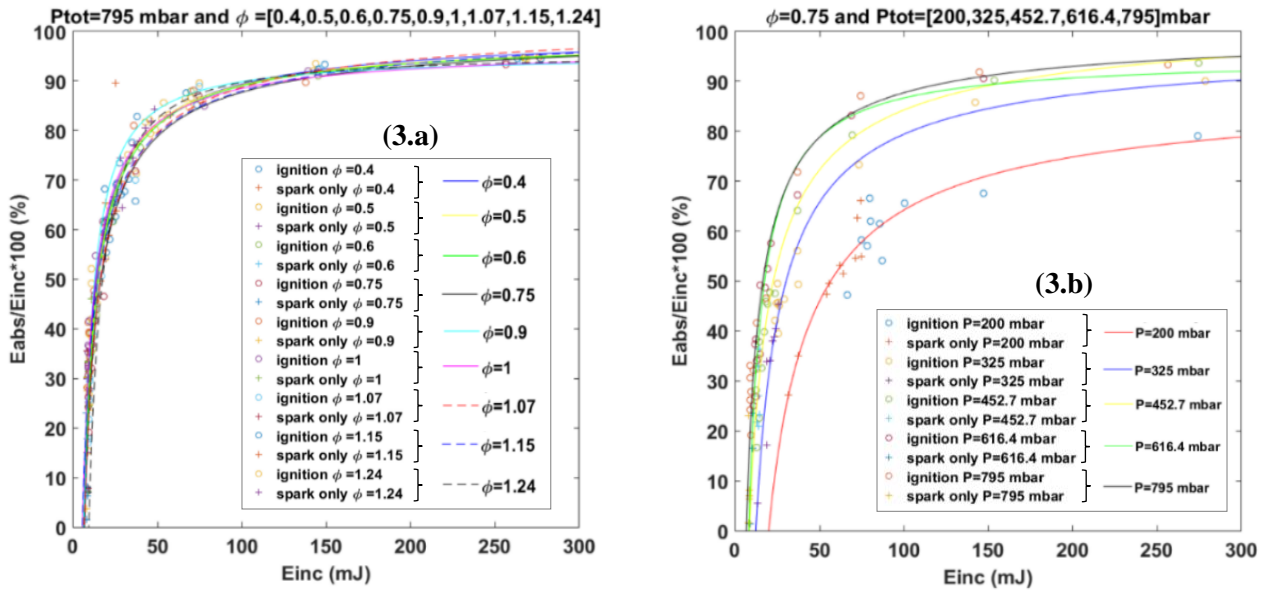


Figure 3. Fraction of absorbed energy [%] (P_{tot} or Φ fixed) vs incident energy E_{inc} [mJ] and fitting curves

Figure 4 underlines the evolution of the fraction of absorbed energy (4.a) and the absorbed energy E_{abs} (4.b) in function of E_{inc} at a given pressure regardless Φ . Figure (4.b) highlights the linearity between absorbed and incident energy. To simplify, one approximates δ equal to 1, which transforms the relation (4) into a linear function and allows to interpolate the value of α and β easily from the fitting curves.

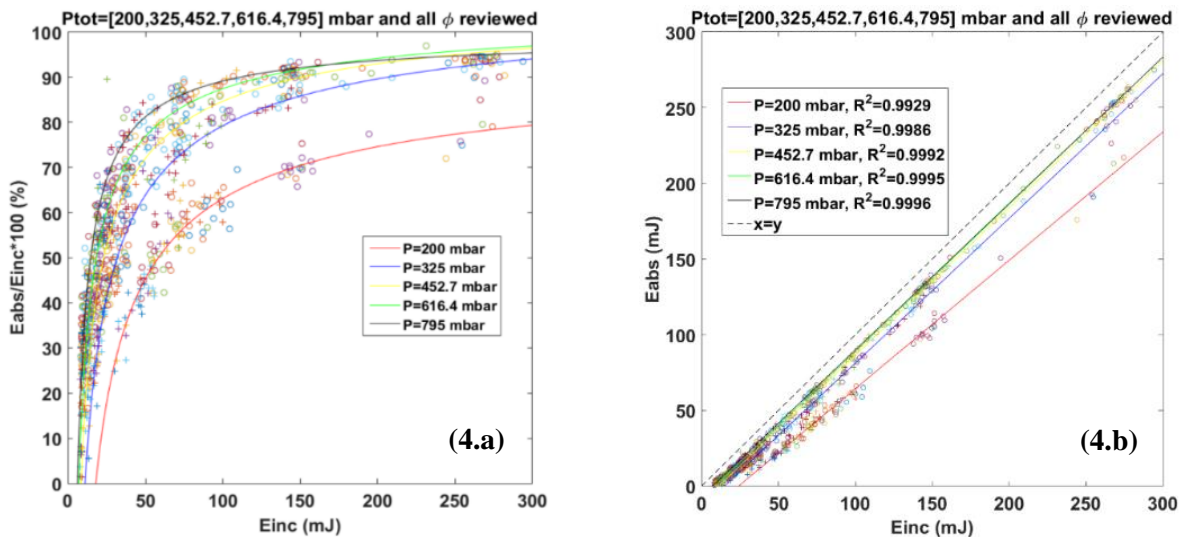


Figure 4. Fraction of absorbed energy [%] and absorbed energy E_{abs} [mJ] vs incident energy E_{inc} [mJ]

The P dependence of β is representative of the cascade collisional ionization process occurring during the breakdown [10]. The relation (5) extrapolated from the fitting curve (5.a) is associated with $R^2 = 0.9983$. This result does not fully match with $\beta_{th} \propto P^{-0.5}$ suggested by [11] for methane/air mixtures and successfully tested in [10] with n-decane/air mixtures. Nevertheless, our approach is quite different, since we focused on E_{50} measurements and not β . Moreover, according to [12] the power factor of pressure is between -0.3 and -0.9 in air.

$$\beta_{mJ} = 5.52 \times P_{bar}^{-0.91} \quad (5)$$

The relation (6) extrapolated from the fitting curve (5.b - 4.b) is associated with $R^2 = 0.996$. This relation could be determined from the maximum fraction of absorbed energy observed (5.b - 4.a) but this method is less accurate. The function (6) significantly increases from 0.2 to 0.35 bar and is quasi-constant afterwards. The last coefficient in α function corresponds to this quasi-constant state, the maximum amount of absorption of incident energy.

$$\alpha = \left(-1.08 \times 10^{-4}\right) \times P_{bar}^{-4.38} + 0.97 \quad (6)$$

Finally, we can establish an empirical modelling of energy deposit for CH₄/Air (20% O₂, 80% N₂) mixtures by laser breakdown and for low pressure:

$$E_{mJ}^{abs} = \left\{ \begin{array}{l} \left(-1.08 \times 10^{-4} \times P_{bar}^{-4.38} + 0.97\right) \times \left(E_{mJ}^{inc} - 5.52 \times P_{bar}^{-0.91}\right) \quad \text{if } E_{mJ}^{inc} > 5.52 \times P_{bar}^{-0.91} \\ 0 \quad \text{else} \end{array} \right\} \quad (7)$$

Figure 6 submits the energy E_{abs} predicted by the empirical model (7) with the observed E_{abs} (targets) during our experimentations with $R^2 = 99.87\%$. This result validates the previous approximations.

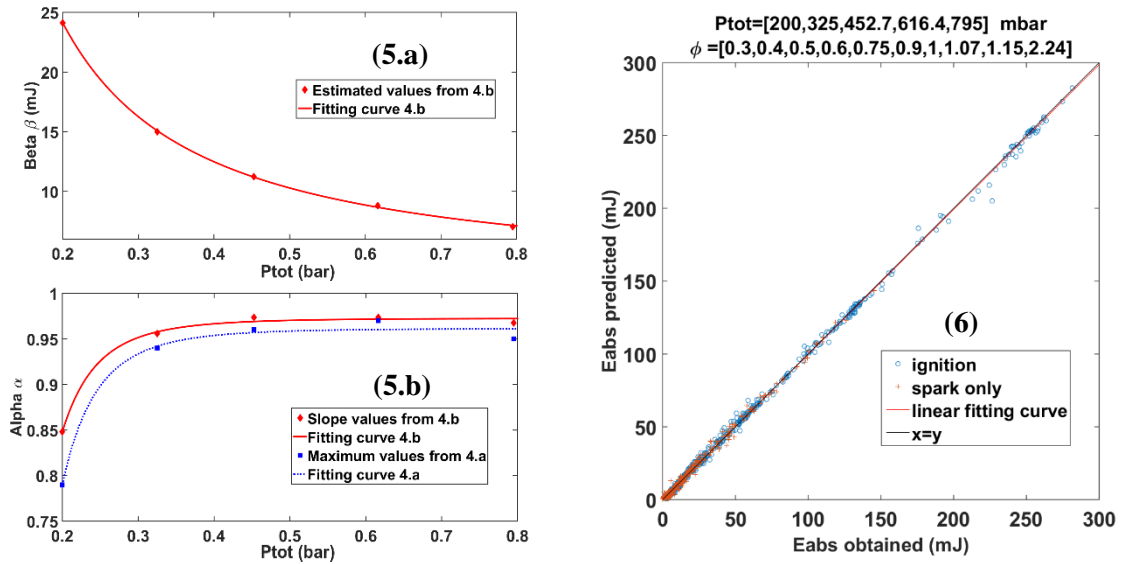


Figure 5. Optimization of α and β in function of the pressure from interpolated values (left)
Figure 6. Absorbed energy predicted by the model vs absorbed energy measured during the tests (right)

5 Conclusion and perspectives

These experimental results report the ignition properties (50% ignition probability) of methane/air (20% O₂, 80% N₂) mixtures at 303 K, for equivalence ratio Φ from 0.3 to 1.24 and static initial chamber pressure ranging from 0.200 to 0.795 bar. For a given equivalence ratio, the initial pressure effect on the E_{50} is mainly significant between 200 and 325 mbar. For a given initial pressure, E_{50} takes the form of a U-shape profile which extends its minimum area with the pressure rise. As in [10] energy absorption is linear in front of incident energy, primarily depends on initial pressure and a similar law for calculating E_{abs} is presented. Next investigations will replicate the tests with air enhanced with oxygen (30% O₂, 70% N₂) for low ranges of static pressures, to better understand the influence of oxygen level in the ignition of methane/air mixtures.

Authors are grateful to ArianeGroup which R&T project on reusable Lox/Methane propulsion supported these study and testing, the CAPRYSES project (ANR- 11-LABX-006–01) funded by ANR through the PIA (Programme d'Investissement d'Avenir) and CNRS FR 776 EPEE for their supports.

References

- [1] Weinrotter M, Kopecek H, Wintner E, Lackner M, Winter F. (2005). Application of laser ignition to hydrogen – air mixtures at high pressures. *International Journal of Hydrogen Energy* 30: 319.
- [2] Weinrotter M, Kopecek H, Tesch M, Wintner E, Lackner M, Winter F. (2005). Laser ignition of ultra-lean methane/hydrogen/air mixtures at high temperature and pressure. *Experimental Thermal and Fluid Science* 29: 569.
- [3] Morsy MH. (2012). Review and recent developments of laser ignition for internal combustion engines applications. *Renew. Sustain. Energy Rev* 16: 4849.
- [4] Xu C, Fang D, Luo Q, Ma J, Xie Y. (2014). A comparative study of laser ignition and spark ignition with gasoline–air mixtures. *Optics & Laser Technology* 64: 343.
- [5] O'Briant SA, Gupta SB, Vasu SS. (2016). Review: laser ignition for aerospace propulsion. *Propulsion and Power Research* 5 (1): 1.
- [6] Kato T, Terakado D, Nanri H, Morito T, Masuda I, Asakawa H, Sakaguchi H, Ishikawa Y, Inoue T, Ishihara S, Sasaki M. (2017). Subscale Firing Test for Regenerative Cooling LOX/Methane Rocket Engine. 7th European Conference for Aeronautics and Space Sciences.
- [7] Dougal J, William-Louis M, Gillard P, Abensur T, Dutheil JP, Boué Y. (2018). Explosion Risk Study On Liquefied Propellants Ejected From A Space Vehicle. 12th ISHPMIE.
- [8] Langlie HJ. (1962). A reliability test method for one shot items. Publication n_U. 1792. Ford Motor Company Aeronutronic.
- [9] Bernard S, Lebecki K, Gillard P, Youinou L, Baudry G. (2010). Statistical method for the determination of the ignition energy of dust cloud-experimental validation. *Journal of Loss Prevention in the Process Industries* 23: 404.
- [10] Rudz S, Tadini P, Berthet F, Gillard P. (2018). Effect of low initial pressures on ignition properties of lean and rich n-decane/air mixtures for laser-induced breakdown. *Combustion Science Technology*.
- [11] Phuoc TX, White FP. (1999). Laser-Induced Spark Ignition of CH₄/Air Mixtures. *Combustion and Flame* 119: 203.
- [12] Sircar A, Dwivedi RK, Thareja RK. (1996). Laser induced breakdown of Ar, N₂ and O₂ gases using 1.064, 0.532, 0.355 and 0.266 μm radiation. *Applied Physics B: Lasers & Optics* 63: 623.